IOPscience iopscience.iop.org

Home Search Collections Journals About Contact us My IOPscience

Micromechanical behaviors of duplex steel: *in situ* neutron diffraction measurements and simulations

This article has been downloaded from IOPscience. Please scroll down to see the full text article.

2008 J. Phys.: Condens. Matter 20 104259

(http://iopscience.iop.org/0953-8984/20/10/104259)

View the table of contents for this issue, or go to the journal homepage for more

Download details:
IP Address: 129.252.86.83
The article was downloaded on 29/05/2010 at 10:44

Please note that terms and conditions apply.

IOP PUBLISHING JOURNAL OF PHYSICS: CONDENSED MATTER

J. Phys.: Condens. Matter **20** (2008) 104259 (7pp) doi:10.1088/0953-8984/20/10/104259

Micromechanical behaviors of duplex steel: *in situ* neutron diffraction measurements and simulations

N Jia[1], Y D Wang[1] and R Lin Peng[2]

[1] School of Materials and Metallurgy, Northeastern University, Shenyang 110004, People's Republic of China

[2] Department of Mechanical Engineering, Linköping University, S-58183 Linköping, Sweden

Received 16 July 2007, in final form 7 August 2007

Published 19 February 2008

Online at stacks.iop.org/JPhysCM/20/104259

Abstract

Recently, much attention has been paid to studying the micromechanical behavior of multiphase materials by virtue of their extensive engineering applications. A strong heterogeneity in stress exists in two-phase materials during loading due to the different thermal expansion coefficients and the respective mechanical properties of each individual phase. For one duplex stainless steel under uniaxial compression, the distributions of microstrains were characterized with the strain response of multiple reflections to the applied external stress for each phase by employing *in situ* neutron diffraction experiments. Based on these, the anisotropic elastoplastic properties of the duplex steel on microscales, i.e. phase size and grain size, were modeled using a two-phase viscoplastic self-consistent (VPSC) model involving lattice rotation (texture evolution). Good agreement between predictions and neutron diffraction measurements was found. The stress partition between phases and orientated grains was discussed to characterize the phase stress and the grain-orientation-dependent stress, thus the particular micromechanical properties of two-phase materials may be explored.

(Some figures in this article are in colour only in the electronic version)

1. Introduction

For multiphase materials now in most extensive engineering applications, internal stresses can arise from differences in thermal expansion ability, yield stress, and stiffness among not only the different phase constituents but also the variously oriented grains. Those stresses characterizing the elastoplastic properties of materials on different microscopic scales, i.e. phase size and grain size, are closely combined with the mechanical processing of components subjected to service. Thus, evaluating the micromechanical behavior for multiphase materials is of great scientific and engineering importance. In recent years, much interest has been triggered on the study of anisotropic micromechanical behaviors of engineering materials by performing diffraction measurements on *in situ* experiments. Accordingly, many efforts are being made to develop numerical and analytical models aiming at the accurate evaluation and reliable prediction of mechanical performances of materials based on these measurements. However, most work is concerned with single-phase materials [1]. As for multiphase materials, only a limited number of measurements and simulations have been accessed [2, 3]. Thus, understanding the grain-to-grain and phase-to-phase interactions in multiphase materials remains ambiguous.

The material used in the current investigation is an austenite–ferrite (γ–α) stainless steel of increasing scientific and engineering interest owning to its exceptional strength and corrosion resistance. In our previous work [4], based on *in situ* neutron diffraction experiments, the distribution of microstrain in this duplex alloy was measured for respective phases. After this, the development of phase stress and grain-orientation-dependent stress during uniaxial compression was described by using one simplified elastoplastic self-consistent (EPSC) model [5], in which the complex interaction between the austenitic and the ferritic phases was ignored and only the grain-to-grain interaction in respective phases was considered. The present work details the application of a newly developed two-phase viscoplastic self-consistent (VPSC) model based on these neutron measurements. Thermal residual stresses,

 © 2008 IOP Publishing Ltd Printed in the UK

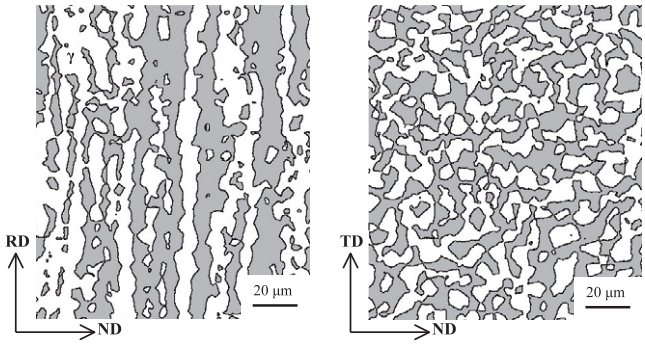

Figure 1. Optical micrographs of the duplex steel in different sample directions.

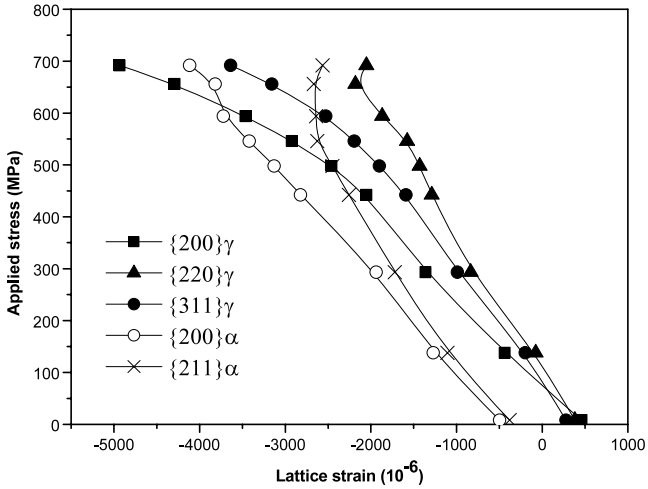

Figure 2. Response of lattice strains to the applied stress along the compression axis for different reflections in the austenite and the ferrite.

initial microstructure and grain orientation, together with texture evolution of the material, are involved in the simulated mechanical process. The elastic and plastic interactions among grains with their specific crystal orientations and mechanical performances are considered within the mixed phases, according to which the stress partition between phases and among orientated grains are characterized by the phase stress and the grain-orientation-dependent stress. Therefore, a clear exploration into the micromechanical behavior of two-phase materials may be obtained.

2. Materials and experiments

The studied stainless steel, SAF 2507, with a nominal chemical composition (wt%) of 25 Cr, 7 Ni, 4 Mo, 1.2 Mn, 0.8 Si and 0.3 N (remainder Fe), was supplied in solution annealed (1100 °C) and water quenched condition. The material thus has an austenitic–ferritic microstructure, which is free from grain boundary carbides and intermetallic phases. The microstructure, that consists of 58% austenite (γ) and 42% ferrite (α) (by volume), is shown by metallographical sections in figure 1. X-ray diffraction reveals that, with the notation of $\{hkl\} \parallel$ ND and $\langle uvw \rangle \parallel$ RD characterizing texture type $\{hkl\}\langle uvw \rangle$, initial textures in γ and α phases are dominated by the $\{110\}\ \langle 001 \rangle$ (Goss) component and the relatively strong $\{100\}\ \langle 001 \rangle$ (Cube) component, respectively. RD is the rolling direction and TD and ND denotes the two radial directions perpendicular to each other. The 0.2% offset yield strength and fracture tensile ductility of the duplex steel are 606 MPa and 30%, respectively.

Neutron diffraction was used to measure the lattice strain distributions of the duplex steel as the cylindrical specimen was undergoing uniaxial compression along its original RD. The lattice strains of the $\{200\}\gamma$, $\{220\}\gamma$ and $\{311\}\gamma$ reflections for the austenite, and the $\{200\}\alpha$ and $\{211\}\alpha$ reflections for the ferrite, were measured in two specimen directions, i.e. the loading and the radial directions, respectively. The specimen was compressed incrementally up to an applied stress higher than its yield strength and subsequently unloaded from the highest load of -700 to -5 MPa, while neutron diffraction spectra were recorded at each loading level. The gauge volume defined by the incident and the diffracted beam slits was limited within the specimen volume (see [4] for details). The interplanar spacing d_{hkl} of the hkl plane was obtained by using Bragg's law. Before this the diffraction peak position was determined by fitting a Gaussian function to the diffraction profile.

The lattice strain ε_{hkl} was calculated from $\varepsilon_{hkl} = (d_{hkl} - d_0)/d_0$, where d_0 is the stress-free interplanar spacing of the specified hkl plane. In the current strain calculation, the lattice constant d_0 is derived by averaging over all the sample directions and hkl planes in each phase and taking into account the stress balance between the γ and α phases.

3. Experimental results and model establishment

Figure 2 shows the evolution of lattice strains, ε_{hkl}, for different $\{hkl\}$ planes measured along the loading direction as a function of the applied compressive stress. It can be seen that before loading the sign of ε_{hkl} is positive for $\{200\}\gamma$, $\{220\}\gamma$ and $\{311\}\gamma$, and negative for $\{200\}\alpha$ and $\{211\}\alpha$, respectively. The strains of different $\{hkl\}$ planes indicate that a thermal residual stress balanced between the two phases was generated during the previous heat-treatment of the as-received material. The signs of strains are in agreement with the fact that the thermal expansion coefficient of the γ phase is larger than that of the α phase [6]. Since lattice strains for the five hkl planes have been experimentally mapped at each constant applied load in various sample directions, the lattice strain distributions along the loading direction to the radial direction of both phases could be obtained, with Ψ defining the angle between the scattering vector and the loading direction. As plotted in figure 3, in the measured results, the negative slope for the γ phase and the positive slope for the α phase indicate the existence of tensile stress and compressive stress in the respective phases along the rolling direction of the as-received material. The linear variation of the lattice strains with $\sin^2\Psi$ indicates a homogeneous strain state in all the sampled populations during the Ψ tilts, meaning that the grain orientation-dependent stress

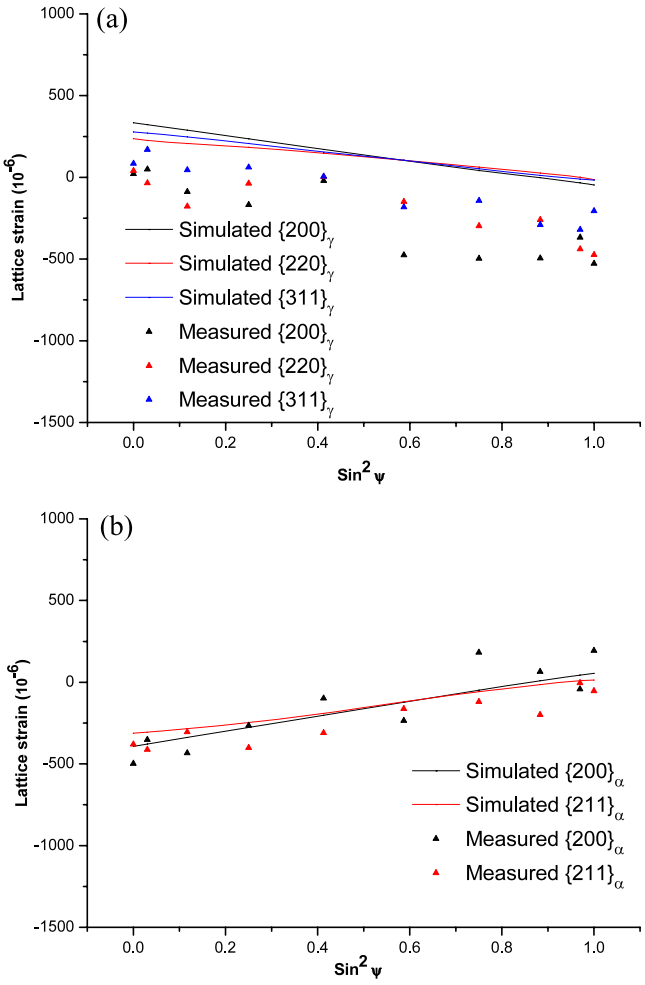

Figure 3. Measured and simulated lattice strain distributions for different reflections in (a) austenite and (b) ferrite, before loading.

may not exist in the as-received material. The discrepancy in the lattice strains between the experimental and the simulated results will be discussed later.

A viscoplastic self-consistent (VPSC) model was implemented to simulate the micromechanical behavior of the studied duplex steel during deformation. In the presented simulation, each grain is considered as an inclusion embedded in a homogeneous equivalent medium mixed with the austenitic and the ferritic grains. The external loading acts as the boundary condition of the deformation and is fulfilled by accommodating stress/strain distributions within the material at the grain level. For each single crystal, the hardening function of its ith slip system is calculated as

$$\tau^{\mathrm{i}}(\Gamma) = \tau_0^{\mathrm{i}} + (\tau_1^{\mathrm{i}} + \theta_1^{\mathrm{i}}\Gamma)\left[1 - \exp\left(-\frac{\theta_0^{\mathrm{i}} \cdot \Gamma}{\tau_1^{\mathrm{i}}}\right)\right], \qquad (1)$$

where Γ is the shear increment accumulated on all systems over the deformation history and τ^{i} is the instantaneous flow stress as a function of Γ. The initial deformation is characterized by τ_0^{i} (the critical resolved shear stress) and θ_0^{i} (hardening rate), while the asymptotic hardening is characterized by τ_1^{i} and θ_1^{i}. To predict the elastoplastic process of the duplex steel, calculations were performed for 2592 and 1877 ellipsoidal inclusions (with the axis ratio of 1:1:3 corresponding to ND, TD and RD) representing grains of austenite (58%) and ferrite (42%). The initial orientations of the crystallites corresponding to the experimental textures are used as the input data for each phase. For the austenitic phase with the fcc crystal structure, slip is considered on the close-packed {111} planes and in the ⟨110⟩ close-packed directions. For the ferritic phase, since there is not a close-packed structure in bcc materials, slip is considered to take place on many slip systems, with the ⟨111⟩ direction in common, i.e. {110}⟨111⟩ and {112}⟨111⟩ are considered in the simulation.

To introduce the initial thermal residual stress into the simulation of the subsequent deformation, a thermal process with the temperature gradient corresponding to the process of water quenching was modeled. The specimen is assumed to be in the hydrostatic state and stress equilibrium is considered between the two phases, i.e.

$$(1 - V_\alpha) \times {}^{\mathrm{tot}}\sigma^{\gamma} + V_\alpha \times {}^{\mathrm{tot}}\sigma^{\alpha} = {}^{\mathrm{M}}\sigma, \qquad (2)$$

where V_α is the volume fraction of the α phase and ${}^{\mathrm{tot}}\sigma^{\gamma}$ and ${}^{\mathrm{tot}}\sigma^{\alpha}$ are the total stresses for the γ and α phases averaged over their constitutive single crystals. ${}^{\mathrm{M}}\sigma$ is the macrostress of the two-phase material, which is zero in these circumstances, as under heat treatment no external stress is applied on the specimen volume.

Also as shown in figure 2, when the load comes to −150 MPa, the strain values of all the lattice reflections become compressive in the axial direction and continue to increase with the increasing applied stress. When the stress is continuously elevated step by step, the evolution of elastic strain varies among the different *hkl* reflections of both phases due to their respective elastic properties. Linear responses of the lattice strains to the applied stress are observed for all the investigated *hkl* planes in the specimen before loading up to −250 MPa, which indicates that the elastic behavior is dominant at this stage in both phases. Because of the similar elastic constants for the α and γ phases [9] (table 1), the same hardening parameters $\theta_0^{(\alpha)}$ and $\theta_0^{(\gamma)}$, that denote the plastic response of the two phases at the onset of microyielding, are used in the simulation. After loading to −500 MPa, the nonlinearity is evident for all the *hkl* planes, indicating that the microscopic yielding has started and the plastic behavior is dominant in both phases. For all the reflections, microscopic yielding occurs below the macroscopic yielding stress of the material (606 MPa) but at different macrostresses among the various grain populations.

These differential yielding points determine the microplastic properties of the individual phases, thus they are used for fitting the critical resolved shear stress τ_0 for the γ and α phases in mechanical simulation. Since the slip planes in the ferrite are not close-packed as in the case of the austenite, higher shear stresses are necessary for slip in ferrite than in austenite. When the loading is applied in the plastically deformed stage and even further, the slope of lattice strain continues to be differential among different crystallographic planes, indicating the different degrees of plastic anisotropy.

Table 1. Single-crystal elastic constants C_{ij}, diffraction elastic constants (E) and Poisson's ratio (ν) for the austenite (γ) and the ferrite (α).

	C_{11} (GPa)	C_{12} (GPa)	C_{44} (GPa)		E (GPa)	ν
				$\{200\}\gamma$	149	0.345
Austenite (γ)	204.6	137.7	126.2	$\{220\}\gamma$	213	0.278
				$\{311\}\gamma$	184	0.309
Ferrite (α)	236.9	140.6	116.0	$\{200\}\alpha$	175	0.331
				$\{211\}\alpha$	225	0.283

Namely, a noticeable nonlinearity for the $\{200\}\gamma$, an insensitive response for the $\{311\}\gamma$ and an upward deviation of linearity for the $\{220\}\gamma$ are observed (figure 2). As for the α phase, the slope for the $\{211\}\alpha$ is obviously higher than that for the $\{200\}\alpha$. Similar observations have been reported based on *in situ* diffraction experiments performed on single-phase austenitic and ferritic alloys [7, 8]. In this range, the lattice strain evolution depends on the relative hardening of the two phases. By fitting the simulation to the experimental slopes of each individual *hkl* plane, the ratio of asymptotic hardening parameters ($\theta_1^{(\alpha)}/\theta_1^{(\gamma)}$) of 0.12 is determined for the austenite and the ferrite. The value of $\theta_1^{(\alpha)} + \theta_1^{(\gamma)}$ mainly influences the slope of the macrostress–strain curve of the two-phase material; thus, the absolute values of the hardening parameters $\theta_1^{(\alpha)}$ and $\theta_1^{(\gamma)}$ could be finally determined by fitting the predicted macrostress–strain flow curve of the duplex steel to the measurements from mechanical tests. It should be stated that, using the present method [3], which is essentially based on neutron diffraction measurements on individual lattice reflections of the respective phases, the initial critical stress and the hardening parameters can be determined independently for the austenite and the ferrite. However, this is rarely straightforward if only conventional mechanical approaches are applied.

4. Discussions

4.1. Response of lattice strains to loading

Figures 4 and 5 show both the simulated and the neutron diffraction measured responses of lattice strains against the macroscopic applied stress, parallel and perpendicular to the loading direction respectively. It can be seen that after the settlement of the model parameters for each phase an excellent agreement between simulation and experimental results could be obtained along the loading direction, which is of especial importance since it proves that the present two-phase self-consistent formula is reliable for generally predicting the interaction between elastically and plastically deformed phases. In both directions for measurements, deviations from an elastic linear response caused by the preferential yielding of some grains with their specific orientations and mechanical properties are predicted far below the macroscopic plasticity for the austenite (∼−250 MPa) and close to the onset of macroscopic yielding for the ferrite (∼−500 MPa), respectively, owing to the fact that the stress redistribution caused by both the grain-to-grain interactions within one phase and phase-to-phase interactions has been involved in modeling the elastic and plastic behavior of the two-phase material. In addition, this nonlinearity in lattice

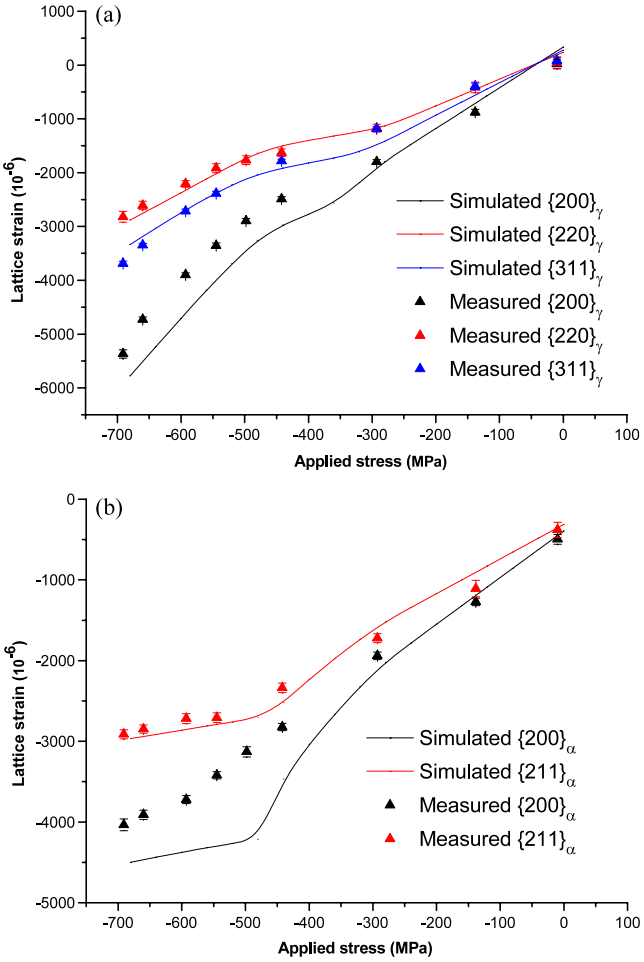

Figure 4. Measured and simulated response of lattice strains to the applied stress along the compression axis for different reflections in (a) austenite and (b) ferrite.

strain response occurs at different macrostresses for one specific family of grains between the two sample directions, i.e. in the axial direction and the transverse direction. This indicates an effect of the diffracting elastic module and Poisson's ratio for one *hkl* lattice plane.

However, the single-peak response in the transverse direction (figure 5) shows some large discrepancies between the simulated and the measured points, although this may be partly explained by the experimental scatter and the inaccurate values of lattice constant d_0. In fact, it is mainly induced by the discrepancy in the initial strains, i.e. the thermal residual strains for most lattice planes, since quite the similar tendencies of lattice strain evolution could be found in the

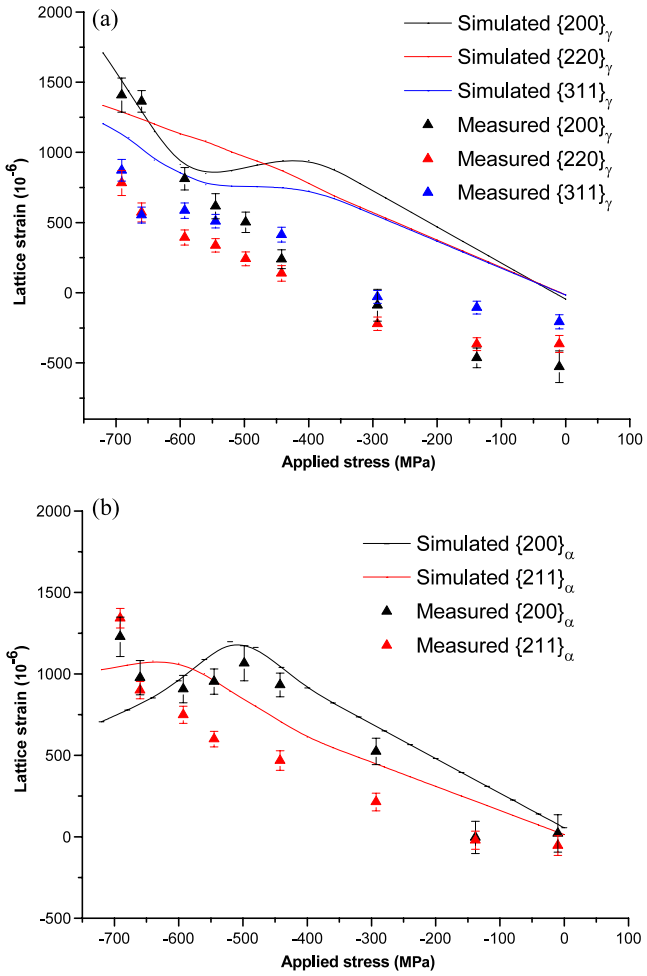

Figure 5. Measured and simulated response of lattice strains to the applied stress perpendicular to the compression axis for different reflections in (a) austenite and (b) ferrite.

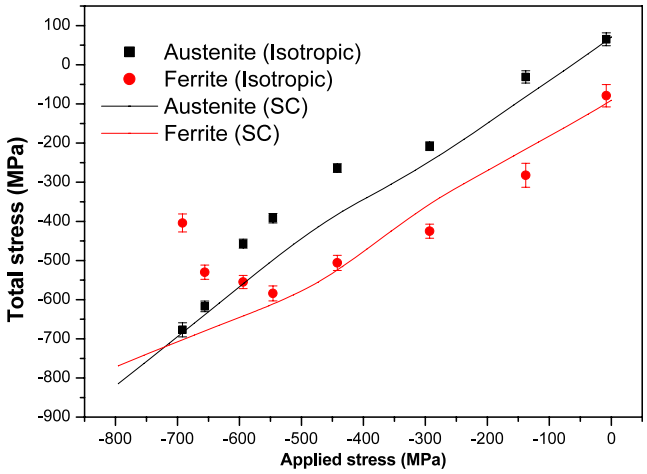

Figure 6. Self-consistent model simulated and isotropic model calculated total stress of each individual phase as a function of the applied stress for the duplex steel.

simulated and the measured results. It is worth noting that the macrostress varies with depth in the material, although it is in equilibrium over the complete specimen. Concerning neutron diffraction experiments, the determined stresses are averages over the irradiated volume. Thus, regarding the measurements in practice, only limited dimension and shape of the specimen which have been defined by slits on the incident and the diffracted beams is selected as the diffracting volume. This means that, before loading, the measured sample volume actually undertakes a residual stresses balanced with the rest of the whole specimen, and this stress is non-hydrostatic on a macroscopic scale [10]. However, this is beyond the consideration in the current simulation of the thermal process prior to loading.

4.2. Development of phase stress and grain-orientation-dependent stress

As for two-phase materials, during elastic and plastic deformation, the stress distribution inside the polycrystals is highly heterogeneous, primarily due to not only the grain orientations but also the variation of phases. Since the accommodation activity of a constituent grain depends directly on its local stress, the deformation of polycrystalline materials depends on the level of accommodation in the phases and grains, which enables us to use the self-consistent method to predict the loading response and the resulting performance among the constituents of two-phase materials. The overall stress and strain states of one grain aggregate could be calculated as the weighted averages of the counterparts over its constitutive grain orientations and shapes.

In another way, based on diffraction experiments, the stress tensor components of one diffracting grain family could be determined from the three measured principal strain tensor components, ε_1, ε_2 and ε_3 (1 denotes the RD, 2 and 3 denote the two orthogonal directions normal to the RD and $\varepsilon_2 = \varepsilon_3$) according to the isotropic model using Hooke's law:

$$\sigma_i = E[\varepsilon_i + \nu(\varepsilon_1+\varepsilon_2+\varepsilon_3)/(1-2\nu)]/(1+\nu), \qquad i = 1, 2, 3 \tag{3}$$

where E is the diffraction elastic constant and ν is Poisson's ratio in the subset of grains with their $\{hkl\}$ crystal planes normal to the scattering vector. All the parameters determined by the Kröner model for the austenite and the ferrite are listed in table 1 [11].

Figure 6 shows the total stress of each individual phase as a function of the applied stress of the duplex steel by using self-consistent simulation and calculation based on the isotropic model. In the isotropic model, calculation is made merely using the lattice strains measured on {311} and {211} reflections for the γ and α phases, respectively. It can be seen that, before loading, the stresses in the γ and α phases are positive and negative, respectively, leading to a phase stress of approximately 150 MPa due to thermal mismatch between the phases. Before loading up to −500 MPa, the stress discrepancy of this thermal origin remains between the phases but decreases with the elevated external stress. Moreover, both the calculations show that the γ phase undertakes less load than the α phase, indicative of the relative hardness of the austenite compared with the ferrite at this stage. The accommodation of the initial (thermal residual) stress with

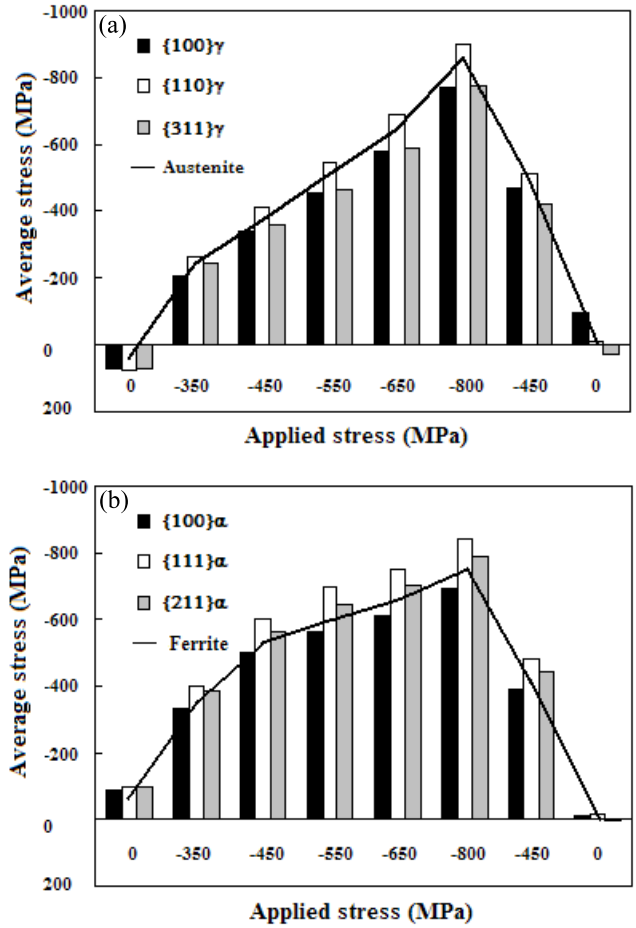

Figure 7. Self-consistent model simulated average stresses for specifically oriented grains along the loading direction as a function of the applied stress during loading and unloading in (a) austenite and (b) ferrite.

the intrinsic elastoplastic properties of each individual phase then acts as the explanation for the decreasing but prominent stress partition between the phases during this period. At approximately −550 MPa, when slipping is initiated in all grains in either phase, the overall stresses of the two phases continue to approach each other but in a much faster manner. An evident decrease in stress partition between the γ and α phases is predicted by both models when macroscopic plastic deformation reaches ∼−650 MPa. After this stage, the phase stress starts to increase again, whereas the γ phase starts to undertake more load than the α phase. The differences between the self-consistent simulation and the isotropic calculation indicate a major contribution of grain-orientation-dependent stresses to phase-to-phase interactions.

To examine the stress redistribution within the duplex steel under loading and unloading, the two-phase self-consistent model simulated average stresses for specifically oriented grains along the loading direction, i.e. ⟨uvw⟩ ∥ RD, are plotted as a function of the applied stress during loading and unloading as shown in figure 7, in which the overall stresses for each individual phase are also indicated.

As seen from the variation of stresses among the orientated grains, before loading, the intergranular microstresses in both phases are very small. With the increasing external stress, moderate grain-orientation-dependent stresses are generated due to the preferential yielding of some plastically soft grains based on the lattice strain distributions as discussed before. At above −550 MPa, when yielding has started in all grains of both phases, the grain-orientation-dependent stresses are significantly developed because of the strong anisotropy of plastic properties among different {*hkl*} reflections in either phase. The largest grain-orientation-dependent stress is found at the maximum load of −800 MPa for both phases, which may be attributed to the strain hardening and texture evolution in the γ and α phases. These simulated results are in accordance with previous investigations on stress distributions relevant to the elastic and plastic anisotropy of single-phase austenite and ferrite materials [12]. The predicted microstresses at unloads (−450 and 0 MPa during unloading), also as presented in figure 7, show that the averaged phase stresses together with the stress partition between the phases decrease, whereas prominent intergranular interaction remains among the different lattice planes in austenite.

As for the neutron diffraction measured results, however, the examination of the heterogeneity in stress within the two-phase material may not be straightforward. Although the nonlinear relationship between lattice strains and $\sin^2\psi$ for each diffracting subset indicates the presence of grain-orientation-dependent stresses of the material undergoing deformation (which are not shown here), the intergranular and interphase interactions could not be quantitatively characterized. The reason is discussed below.

The total stress in the γ phase, ${}^{\mathrm{tot}}\sigma^{\gamma}$, is the sum of the macrostress, ${}^{\mathrm{M}}\sigma$, and a microstress component, ${}^{\mu}\sigma^{\gamma}$, i.e.

$$ {}^{\mathrm{tot}}\sigma^{\gamma} = {}^{\mathrm{M}}\sigma + {}^{\mu}\sigma^{\gamma}. \tag{4} $$

As for the phase stresses, ${}^{\mu}\sigma^{\gamma}$ and ${}^{\mu}\sigma^{\alpha}$, in the γ phase and the α phase, considering a stress balance between the two phases in the duplex steel, it holds that

$$ (1 - V_{\alpha}) \times {}^{\mu}\sigma^{\gamma} + V_{\alpha} \times {}^{\mu}\sigma^{\alpha} = 0 \tag{5} $$

where V_{α} is the volume fraction of the α phase. If the total stress for each phase is determined from the diffraction measured strains in individual *hkl* reflections by equation (3), then macrostress and phase stresses can be separated by employing equations (4) and (5). However, it should be made clear that the stresses determined by diffraction are averages over the irradiated volume. Thus, the value of total stress depends on different lattice reflections, meaning that the macrostress and phase stress obtained with this method depend on the selection of *hkl* planes in each phase. That is to say, the difference in stress obtained from the different combinations of the *hkl* in each phase reflects the grain orientation-dependent stresses existing in two-phase materials, and this intergranular anisotropy in stress could not be obtained directly using the isotropic model unless a comparison is made among the calculations based on various combinations of lattice reflections for the γ phase and the α phase.

In addition, due to the large effect of the different lattice reflections on their stress/strain states, the elastic and

plastic anisotropy of the studied material highly depends on the selection of the crystallographic planes in diffraction experiments. If only the neutron measured *hkl* planes, i.e. {200}, {220} and {311} for the γ phase and {200} and {211} for the α phase, are considered in stress calculation and based on the $\sin^2\psi$ diffraction method, one may conclude that the grain orientation-dependent stresses in the austenite are stronger than those in the ferrite after an analysis of the mean phase stress ($\sigma_{11}^{ph} - \sigma_{33}^{ph}$) distribution as a function of the applied stress for each phase [13]. However, the self-consistent simulation provides us with complete information on intergranular interactions along various directions (figure 7), showing that comparable grain orientation-dependent stresses have also been developed in the ferrite between the {100} and {111} reflections when the specimen is under plastic deformation.

5. Conclusions

Neutron diffraction has been employed to measure the lattice strain distributions for respective phases in a duplex steel under uniaxial loading. Based on those experimental data, heterogeneous stresses of the two-phase alloy are simulated using a two-phase viscoplastic self consistent model. The model has involved the elastic and plastic interactions among grains of their specific crystal orientations and mechanical properties, together with texture evolution of both phases. However, further work is still required to take into account the influence of initial macrostresses on the deformation of both phases in the duplex steel to precisely capture the experimental results. Correlations between the neutron data and the developed model are discussed, providing a good understanding of the self-consistent simulation that manifests the micromechanical behaviors of two-phase alloys.

Acknowledgments

This work is supported by the National Natural Science Foundation of China (grant No 50671022) and the Swedish Research Council in the frame of the SIDA project (grant No 348-2004-3475).

References

[1] Karaman I, Sehitoglu H, Maier H J and Chumlyakov Y I 2001 *Acta Mater.* **49** 3919
[2] Daymond M R and Priesmeyer H G 2002 *Acta Mater.* **50** 1613
[3] Baczmański A and Braham C 2004 *Acta Mater.* **52** 1133
[4] Jia N, Peng R L, Wang Y D, Chai G C, Johansson J, Wang G and Liaw P K 2006 *Acta Mater.* **54** 3907
[5] Hutchinson J W 1970 *Proc. R. Soc. Lond.* A **319** 247
[6] Harjo S, Tomota Y and Ono M 1999 *Acta Mater.* **47** 353
[7] Daymond M R, Tomé C N and Bourke M A M 2000 *Acta Mater.* **48** 553
[8] Pang J W L, Holden T M and Mason T E 1998 *J. Strain Anal.* **33** 373
[9] Simmons G and Wang H 1971 *Single Crystal Elastic Constants and Calculated Aggregate Properties: A Handbook* (Cambridge, MA: MIT Press)
[10] Martinez-Perez M L, Mompean F J, Ruiz-Hervias J, Borlado C R, Atienza J M, Garcia-Hernandez M, Elices M, Gil-Sevillano J, Peng R L and Buslaps T 2004 *Acta Mater.* **52** 5303
[11] Ledbetter H M 1984 *Phys. Status Solidi* a **85** 89
[12] Dye D, Stone H J and Reed R C 2001 Current opinion in solid state and materials *Science* **5** 31
[13] Peng R L, Wang Y D, Chai G C, Jia N, Johansson S and Wang G 2006 *Mater. Sci. Forum* **524** 917